Development and characterization of coatings on Silicon Pore Optics substrates for the ATHENA mission

Desiree Della Monica Ferreira[a], Anders C. Jakobsen[a], Finn E. Christensen[a], Brian Shortt[b], Michael Krumrey[c], Jørgen Garnæs[d], Ronni B. Simonsen[a]

[a]DTU Space, Technical University of Denmark, Elektrovej, bygn. 327, 2800, Denmark
[b]European Space Agency (ESTEC), Keplerlann 1, PO Box 299, 2200 AG, Noordwijk, Netherlands
[c]Physikalisch-Technische Bundesanstalt (PTB), Abbestraße 2-12, 10587 Berlin, Germany
[d]Danish Fundamental Metrology Ltd., Matematiktorvet 307, 2800, Denmark

ABSTRACT

We present description and results of the test campaign performed on Silicon Pore Optics (SPO) samples to be used on the ATHENA mission. We perform a pre-coating characterization of the substrates using Atomic Force Microscopy (AFM), X-ray Reflectometry (XRR) and scatter measurements. X-ray tests at DTU Space and correlation between measured roughness and pre-coating characterization are reported. For coating development, a layer of Cr was applied underneath the Ir/B_4C bi-layer with the goal of reducing stress, and the use of N_2 during the coating process was tested in order to reduce the surface roughness in the coatings. Both processes show promising results. Measurements of the coatings were carried out at the 8 keV X-ray facility at DTU Space and with synchrotron radiation in the laboratory of PTB at BESSY II to determine reflectivity at the grazing incidence angles and energies of ATHENA. Coating development also included a W/Si multilayer coating. We present preliminary results on X-ray Reflectometry and Cross-sectional Transmission Electron Microscopy (TEM) of the W/Si multilayer.

1. INTRODUCTION

The ATHENA (Advanced Telescope for High Energy Astrophysics) mission is an X-ray observatory under study by ESA. The ATHENA mission concept consists of two X-ray telescopes, with a focal length of 11.5 m, and is based on Silicon Pore Optics (SPO)[1] mirror modules to focus incoming X-ray photons at low grazing incidence angles. In short, a SPO substrates is a ribbed and angular wedged Si wafer plate that stacks directly on top of another plate by means of covalent Si-Si bonding. Photoresist stripes are applied to the substrates as part of the masking process. Each mirror module consists of 2×68 reflecting SPO substrates, set to allow for double reflection of X-rays.

According to the current design, each X-ray telescopes onboard ATHENA consist of 33320 SPO plates. High throughput in the energy range between 0.1 and 10 keV depends critically on the performance of the mirror coatings.[2] The coating recipe adopted as baseline for ATHENA is a Ir/B_4C bi-layer and the same coating is adopted for all mirror modules at all radii.

It is important that both the SPO substrates and coatings perform optimally. The pre-coating characterization allows for assessment of the performance of the SPO substrates. A coating development campaign provides the insight on the possible process improvements to produce coatings with optimal performances.

Further author information:
Send correspondence to:
Desiree Della Monica Ferreira, e-mail: desiree@space.dtu.dk
Anders C. Jakobsen, e-mail: jakobsen@space.dtu.dk

2. PRE-COATING CHARACTERIZATION

2.1 Atomic Force Microscopy (AFM)

An atomic force microscope gives a direct image of the surface topology by raster scanning a sharp tip over the surface with a non-destructive force. The AFM measurements were carried out by Danish Fundamental Metrology Ltd. The microscope used is a metrology atomic force microscope, where the tip is scanned over the surface using piezoelectric flexures equipped with capacitive distance sensors.

The sensitivity of the capacitive distance sensors along the XY-plane is traceable to an international standard, in terms of a two dimensional grating calibrated by laser diffraction measurements. The sensitivity at the Z-direction is also traceable to a international standard in terms of a step height calibrated by an atomic force microscope equipped with laser interferometers.[3]

All AFM measurements were carried out in dynamic resonant tapping mode, using single crystal silicon cantilevers. The measurement uncertainty is estimated to be 0.1 nm for the recorded profile height. This estimate contains contributions from the calibration method, the reference standards used, the environmental conditions, and from the object being measured (e.g. deformation). The AFM measurements considered in this study are first order line wise corrected along the X-axis and are suitable for 1D PSD analysis.

2.1.1 AFM of SPO samples

The two SPO samples, with and without resist stripes, considered in this study are standard, wedged and ribbed SPO plates, measuring 65.7×65.7mm. For the sample containing resist stripes, the AFM measurement was carefully set to measure the region in between the resist stripes.

Figures 1, 2 and 3 show the AFM images of the SPO sample without resist stripes. The measurements at three different positions (spot 1, 2 and 3) are shown for image sizes of $0.1\times0.1\mu$m, $1\times1\mu$m and $10\times10\mu$m, respectively.

Figures 4, 5 and 6 show the AFM images of the SPO sample with resist stripes. The measurements at three different positions (spot 1, 2 and 3) are shown for image sizes of $0.1\times0.1\mu$m, $1\times1\mu$m and $10\times10\mu$m, respectively.

2.1.2 1 Dimensional power-spectral-density analysis (1D PSD)

The average 1D PSD function along the X-axis is computed from the surface AFM data using the TOPO software.[4] TOPO computes the 1D PSD function along every line in the X direction of the surface data, and then computes the averages in X of the 1D PSD functions.[4]

Figures 7 and 8 show the average 1D PSD functions combining the data from the three different scan scales for each of the spots measured on the SPO samples without and with resist stripes, respectively.

To assess the surface roughness of the SPO samples, we compute the root-mean-square (rms) surface roughness using the TOPO software functions.[4]

The rms surface roughness σ, is define as

$$\sigma = \sqrt{2 \int_{f_1}^{f_2} S(f) df} \ , \tag{1}$$

and it is computed from the average 1D PSD function S(f).

The frequency range considered for the computation of the rms surface roughness via equation 1 is between 0.01nm^{-1} and 1nm^{-1} for all PSD functions. We note that noise from capacitive sensors and from surroundings can contribute to the 1D PSDs for some height frequencies, and may contribute to the rms surface roughness values computed. A methodology for removing those noise peaks is under investigation and will be applied to further analysis.
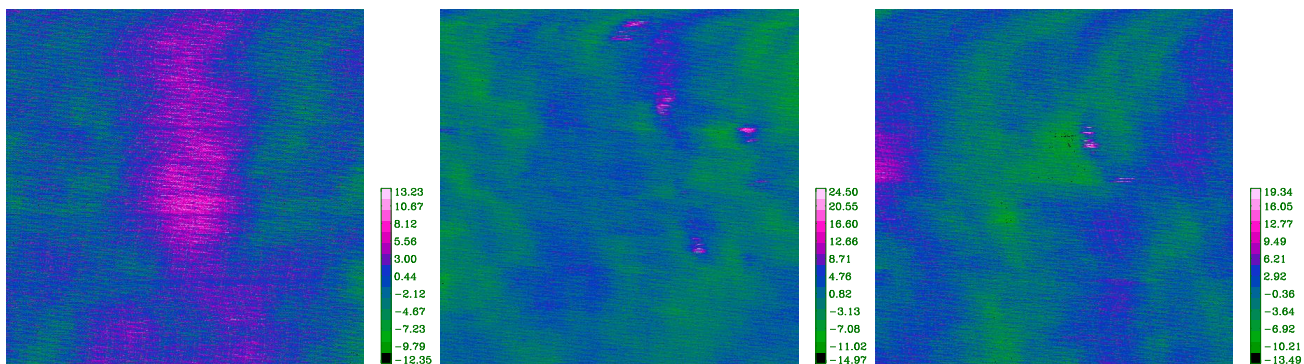
Figure 1. Uncoated SPO sample WITHOUT resist: AFM image, 0.1×0.1μm scan size, measurements on three different spots. Values listed in Å.
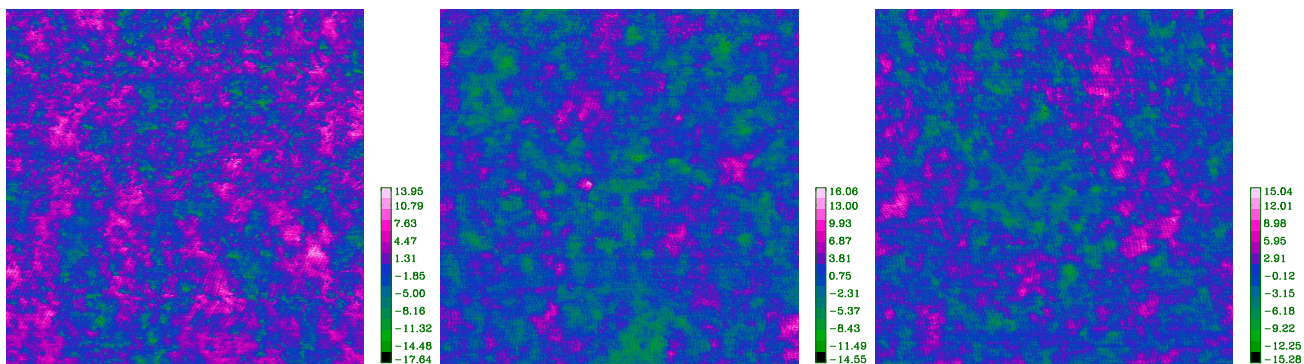

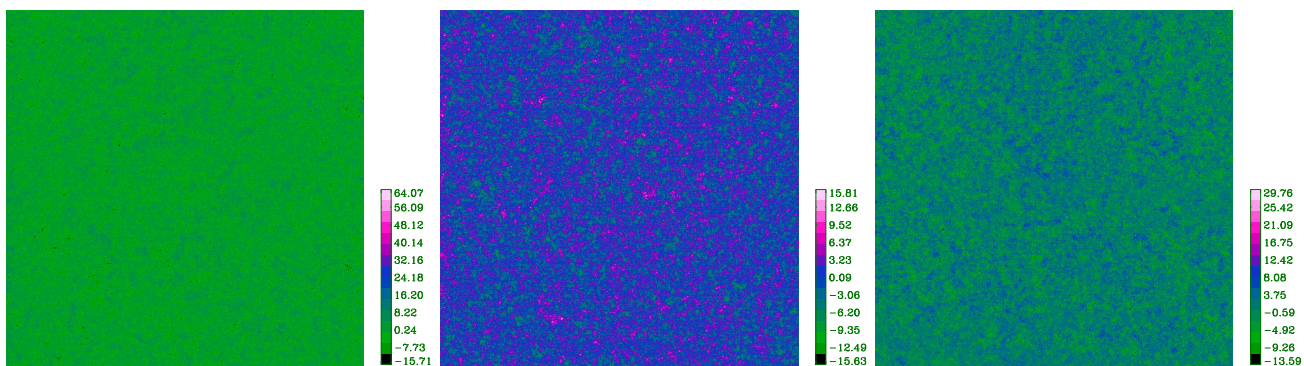Figure 2. Uncoated SPO sample WITHOUT resist: AFM image, 1×1μm scan size, measurements on three different spots. Values listed in Å.

Figure 3. Uncoated SPO sample WITHOUT resist: AFM image, 10×10μm scan size, measurements on three different spots. Values listed in Å.

22.07
18.24
14.41
10.59
6.76
2.94
-0.89
-4.72
-8.54
-12.37
-16.19

10.31
8.26
6.20
4.14
2.09
0.03
-2.02
-4.08
-6.13
-8.19
-10.24

23.99
19.13
14.26
9.40
4.54
-0.33
-5.19
-10.05
-14.92
-19.78
-24.64
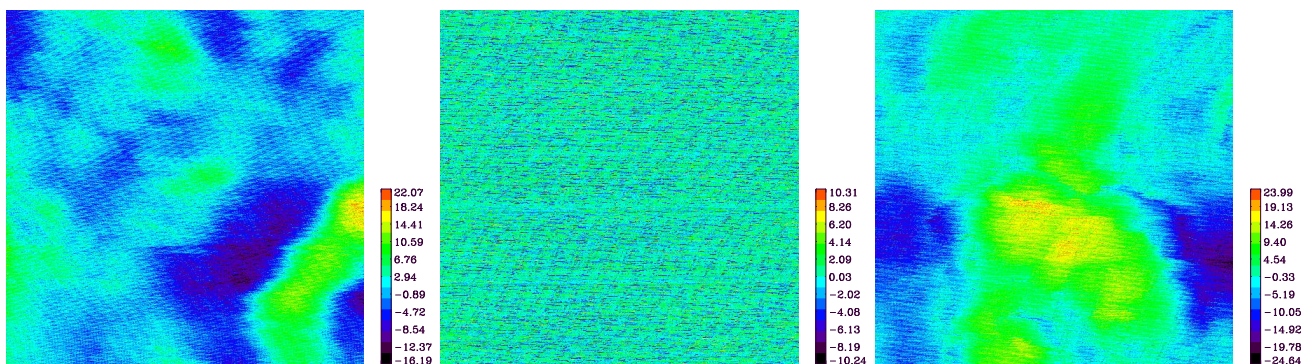
Figure 4. Uncoated SPO sample WITH resist: AFM image, $0.1 \times 0.1 \mu$m scan size, measurements on three different spots. Values listed in Å.

60.78
52.59
44.40
36.20
28.01
19.82
11.63
3.44
-4.75
-12.95
-21.14

9.74
7.85
5.96
4.07
2.18
0.29
-1.60
-3.49
-5.38
-7.27
-9.16

70.52
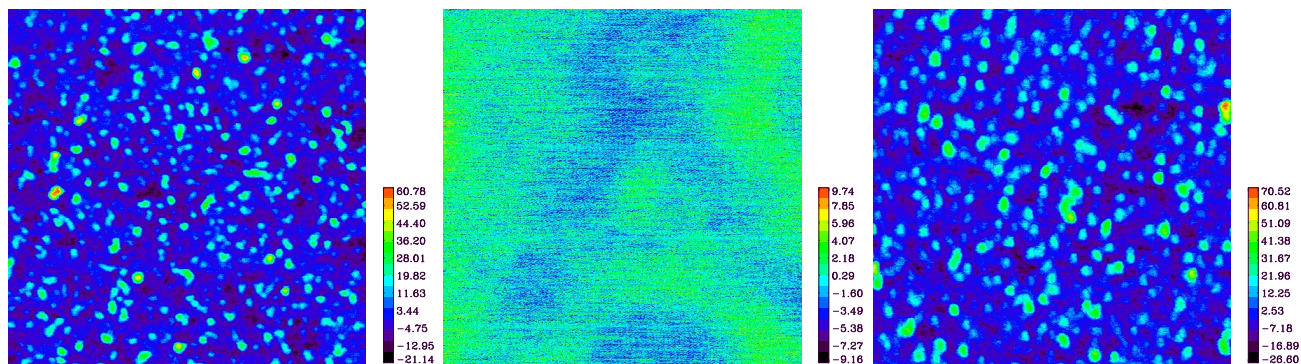60.81
51.09
41.38
31.67
21.96
12.25
2.53
-7.18
-16.89
-26.60

Figure 5. Uncoated SPO sample WITH resist: AFM image, $1 \times 1 \mu$m scan size, measurements on three different spots. Values listed in Å.
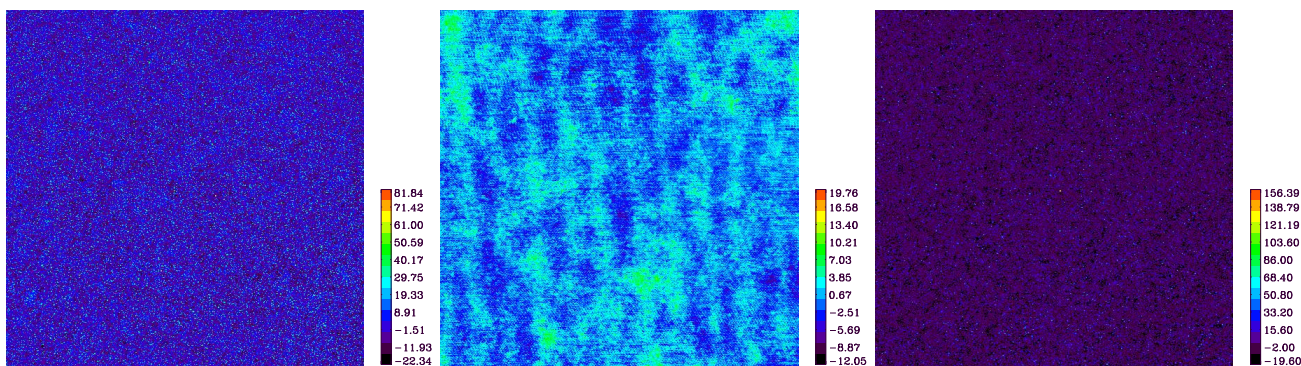
81.84
71.42
61.00
50.59
40.17
29.75
19.33
8.91
-1.51
-11.93
-22.34

19.76
16.58
13.40
10.21
7.03
3.85
0.67
-2.51
-5.69
-8.87
-12.05

156.39
138.79
121.19
103.60
86.00
68.40
50.80
33.20
15.60
-2.00
-19.60

Figure 6. Uncoated SPO sample WITH resist: AFM image, $10 \times 10 \mu$m scan size, measurements on three different spots. Values listed in Å.
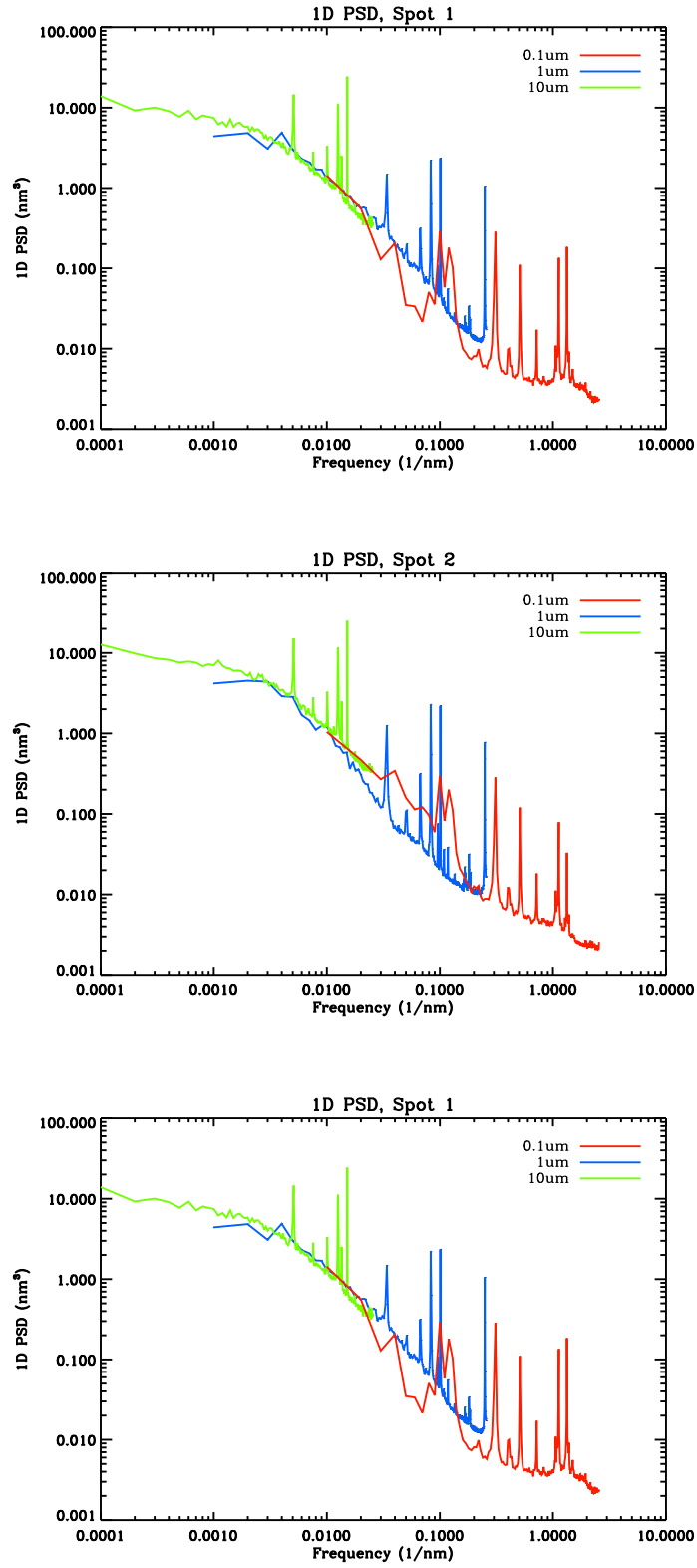
Figure 7. Uncoated SPO sample WITHOUT resist: 1D PSD, data from the three different scan sizes combined.
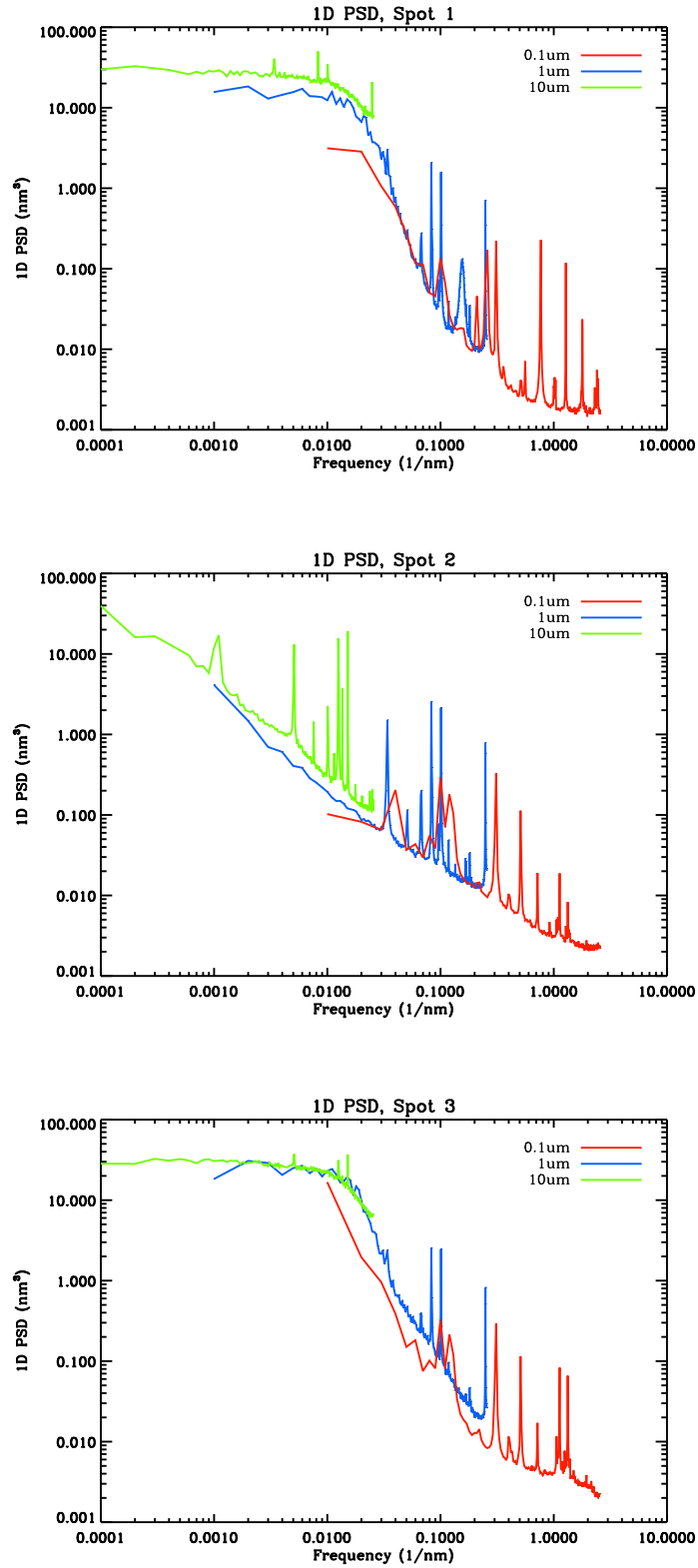
Figure 8. Uncoated SPO sample WITH resist: 1D PSD, data from the three different scan sizes combined.

Sample	Position	Scan size [μm]	σ [Å]
SPO without resist	spot 1	0.10×0.10	2.29
SPO without resist	spot 2	0.10×0.10	2.61
SPO without resist	spot 3	0.10×0.10	2.53
SPO with resist	spot 1	0.10×0.10	3.61
SPO with resist	spot 2	0.10×0.10	2.15
SPO with resist	spot 3	0.10×0.10	3.37
SPO without resist	spot 1	1.00×1.00	1.73
SPO without resist	spot 2	1.00×1.00	2.06
SPO without resist	spot 3	1.00×1.00	2.10
SPO with resist	spot 1	1.00×1.00	6.07
SPO with resist	spot 2	1.00×1.00	1.82
SPO with resist	spot 3	1.00×1.00	7.11
SPO without resist	spot 1	10.0×10.0	1.73
SPO without resist	spot 2	10.0×10.0	1.74
SPO without resist	spot 3	10.0×10.0	1.72
SPO with resist	spot 1	10.0×10.0	6.44
SPO with resist	spot 2	10.0×10.0	1.30
SPO with resist	spot 3	10.0×10.0	6.27

Table 1. Rms roughness computed from AFM of the two SPO samples.

2.1.3 Preliminary AFM results

The values of rms surface roughness derived in this study are listed in table 1. The AFM images, 1D PSD functions and rms surface roughness for the SPO sample without resist stripes at different measurements positions, are similar and consistent with each other, while this is not the case observed for the SPO sample with resist stripes.

The discrepancies observed in the analysis of the SPO sample with resist stripes indicates a non-homogeneous surface and present structures consistent with particulate contamination. Further AFM measurements of uncoated and coated SPO substrates are ongoing in other to clarify the discrepancies observed here.

2.2 Reflectivity and scatter measurements

Three different substrates were tested at DTU Space using X-ray Reflectometry (XRR) at 8 keV, these are: one pure Si wafer piece, one SPO with wedge and with resist stripes and one SPO with wedge and without resist stripes. Additional measurements were performed with synchrotron radiation at the four-crystal monochromator beamline of PTB at BESSY II in Berlin. The beamline provides monochromatic radiation from 1.75 keV to 10 keV with high spectral purity.[5] The samples were mounted in a UHV X-ray reflectometer that enables all 6 degrees of freedom for sample alignment. For one SPO sample without resist, detector scan at fixed energy and incidence angle as well as energy scans at fixed angles were performed.

The results from XRR measurements at DTU Space and the difference in surface roughness for the three substrates are shown in figure 9. Results on the surface roughness obtained by fitting the XRR data are listed in table 2.

The substrate without resist is a raw Si wafer piece with a SiO_x wedge layer. The angular wedging and the subsequent damage etching are responsible for the increased roughness from 0.25 nm to 0.45 nm. The addition of resist stripes further increases the roughness by 0.05 nm in between the stripes.

The energy scan at fixed angle of a SPO substrate without resist is shown in figure 10. The IMD model is comparable to the data with a slight offset. This might be caused by a figure error, the incident beam has a divergence of 43 arc seconds and this will lead to the broadening of edge observed, furthermore, the stochiometry of the wedge material deposited (SiO_x) may not be well described by the SiO model considered. In the IMD model, the wedge material is assumed to be SiO and the roughness $\sigma = 0.45$ nm.

Substrate type	Surface roughness
Raw silicon	0.25 nm
SPO substrate, no resist	0.45 nm
SPO substrate, with resist	0.5 nm

Table 2. Surface roughness obtained by fitting the data using the IMD software.
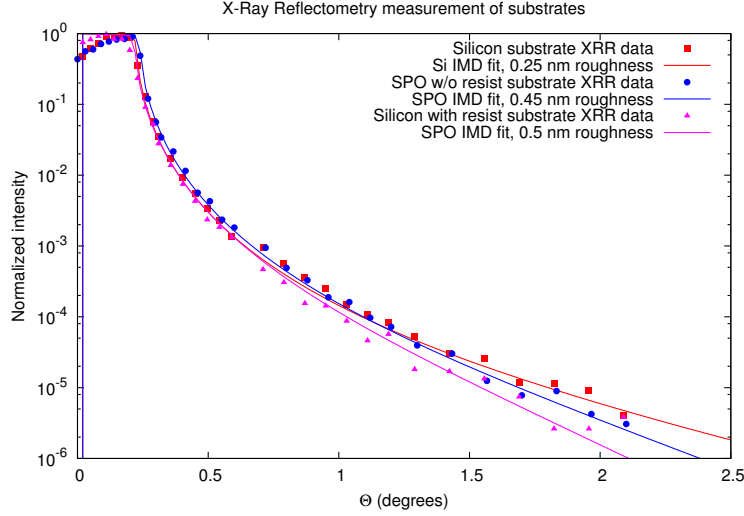

Figure 9. Comparison between XRR of SPO substrate with resist (triangles), SPO substrate without resist (circles) and raw Si wafer (squares) using a Cu K$_\alpha$ 8 keV rotating anode. The data is compared to IMD models (solid lines).

Scatter measurement was carried out on the SPO substrate without resist stripes at fixed angle of $\theta = 0.4^o$ and energy E = 8 keV, and it is shown in figure 11. The uncoated substrate shows little scattering, with 5.5 orders of magnitude needed to see the scatter part. Scatter measurements were also performed at DTU Space on SPO substrates within 4 orders of magnitude and no scatter could be observed.
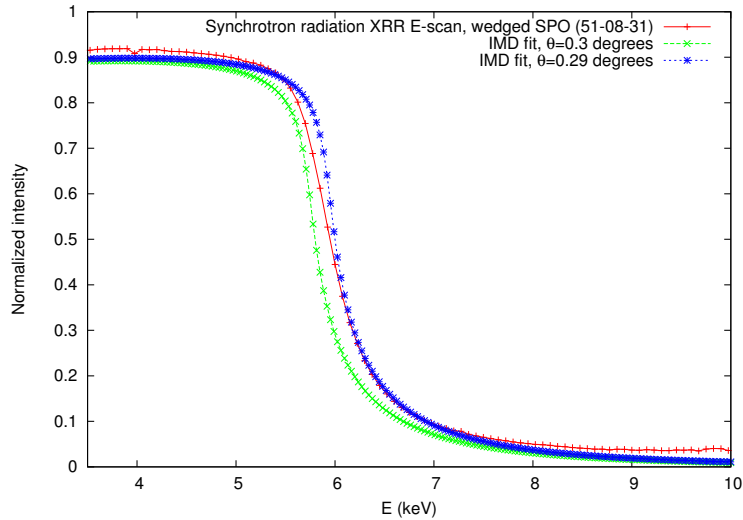

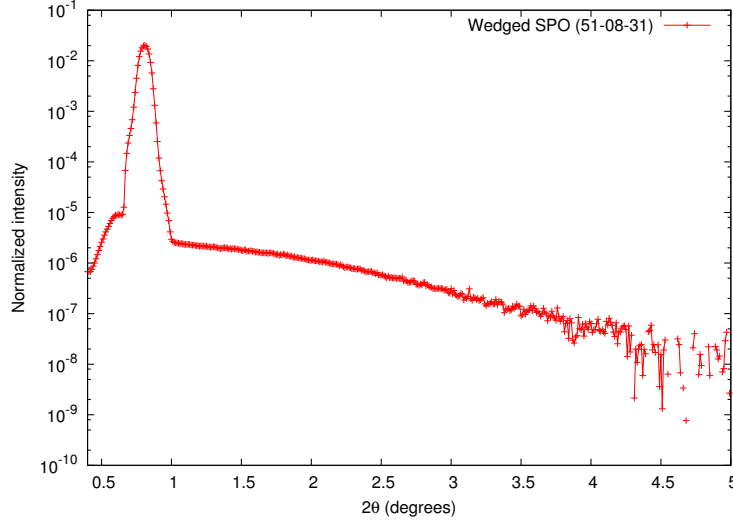Figure 10. X-ray energy scan of SPO substrate w/o resist at $\theta = 0.3^o$. Two IMD models are compared to the X-ray data.

Figure 11. X-ray scatter measurement (background subtracted) of uncoated wedged SPO substrate without resist. Incident angle $\theta = 0.4^o$, energy E = 8 keV. Yoneda shoulder[6] is visible on the left side of the specular peak. Synchrotron radiation measurements taken at the four-crystal monochromator beamline of PTB at BESSY II.

3. COATING CHARACTERIZATION

3.1 Coated samples

Considering the ATHENA current coating baseline design, one SPO plates with resist stripes was coated along with two raw Si wafer pieces and a stress sample. The SPO plate was coated for XRR measurements both with synchrotron radiation in the laboratory of PTB at BESSY II and using a Cu K_α 8 keV rotating anode at the DTU Space. The Si wafer pieces were produced for XRR measurements and adhesion tests.

Initial environmental tests were performed and we observe no degradation on the tri-layer baseline coating. A thorough test campaign will be performed as part of the characterization of the optimized coating design.[2]

A considerable downside of using Ir/B_4C bi-layers in the ATHENA optics is the high stress in sputtered Ir thin films. The stress has shown to cause the film to disintegrate during resist removal after coating using acetone.

To reduce stress we produced test coatings of Ir/B_4C with a Cr undercoat. The required Cr layer thickness is dependent on the Ir thickness. For ATHENA baseline of 10 nm Ir, the optimum Cr thickness applied was of 10 nm. The surface roughness of the Cr layer is considerable ($\approx$ 1 nm), but X-ray Reflectometry results suggest that Ir/B4C bi-layer deposited on top of the Cr shows a roughness of 0.65 nm. This is a degradation in smoothness from 0.45 nm roughness for Ir/B4C without a Cr under layer.

To reduce stress and roughness in the coatings, a possible solution could be the introduction of N_2 gas during sputter deposition. Earlier results[7] have shown that small amounts of nitrogen gas can reduce the interface roughness of some materials.

Preliminary test coatings at DTU Space using N_2 gas during deposition of a Ir/B4C bilayer shown a moderate reduction of stress and surface roughness. The parameters for improvement are limited in the case of reactive gas sputter deposition in DC magnetron sputtering chambers as only the N_2 concentration can be changed and only between 0% and 30%. At higher concentrations, the N_2 molecules will adsorb to the target surface and create insulating regions, so-called target poisoning, which induces arcing that can cause the cathodes to shorten.

Coatings using N_2 presented here have been deposited using a mixture of 10% N_2 and 90% Ar at a total pressure of 2.8 mTorr.

The use of a Pt/B4C bi-layer as an alternative material combination to the Ir/B_4C baseline is under investigation.

Sample	SR XRR spot 1	SR XRR spot 2	SR XRR spot 3	DTU Space 8 keV	SR XRR Nitrogen
Cr/Ir/B$_4$C tri-layer	6.60	6.95	7.47	8.52	1.45

Table 3. Ir/B$_4$C interface roughness derived from X-ray data. Values listed in Å.

3.2 Adhesion qualification tests

Adhesion of the coatings was tested according to ISO9211-4 standard. The ATHENA baseline coating design was tested using scotch tape. By firmly attaching the tape to the surface and quickly ripping the tape off, a consistent test of the coating adhesion was completed. The Ir/B$_4$C bilayer proved able to withstand the removal of the tape.

3.3 Coating stress

The stress of the coating on the substrate was tested. A Dektak 150 Stylus profiler was used to twice measure the profile along the sample before a coating. After the coating the sample was measured again to see any change in the deflection of the sample due to the coating. By factoring in the thickness of the coating, a calculation of the compressive and tensile stress of the film was obtained. The sample used were 5 x 80 mm Si wafer pieces.

The baseline Ir/B$_4$C shows $\approx$ -4000 MPa of compressive stress and using N$_2$ can lower that value to $\approx$ -1600 MPa. Using a Cr undercoat on the baseline Ir/B$_4$C will decrease the stress significantly,[8,9] although there is some variation in the results. Latest results for a Cr/Ir/B$_4$C coating, with at 10 nm Cr undercoat, vary between 100 MPa and -1000 MPa in total stress.

As mentioned in section 3.2, the coating showed good adhesion to the substrate even when stress is high. The main problem of stress in optical coatings are the tendency of low adhesion and the possibility of bending the substrate, which for X-ray optics would decrease the efficiency of the optic. Since the coating shows good adhesion and since a stack of SPO substrates have little or no tendency to bend, the stress of the baseline coating is not likely be an issue.

3.4 X-ray reflectivity

Coating characterization using XRR was performed on the tri-layer Cr/Ir/B$_4$C. The XRR data collected at the laboratory of PTB at BESSY II and at the 8 keV X-ray facility at DTU Space are fit in order to check how well the coating recipes were produced, to evaluate the interface roughnesses and to compare the theoretical predictions to the actual performance of the produced coatings.

At the laboratory of PTB at BESSY II, the measurements were taken at three different spots for each coated sample and at one spot for the sample coated using Nitrogen. The XRR data is shown in figure 12. The grazing incident angle for XRR data is 0.619°.

The theoretical models for each coating were fit to the XRR data using the IMD software.[10] For the tri-layer coating, the model parameters allowed to vary are: layer thickness for each individual layer and roughness for each layer interface. The XRR data along with the best fit curves is presented in figure 13.

The roughness values for the Ir/B$_4$C interface obtained from fitting XXR data are listed in table 3 where we observe a significant reduction on roughness for the sample coated using N$_2$.

Introducing N$_2$ gas while coating will change coating rates for all materials. When introducing 10% N$_2$ while coating, low-Z materials will increase the coating rate by up to a factor of three and high-Z materials will have a 10-30% lower coating rate. At other reactive gas concentrations, the change in sputter rate will differ. For that reason, coating exact d-spacings for every material type requires thorough recalibration compared to non-reactive sputtering. Further investigation is necessary to understand the impact of nitrogen use on the coating performance.
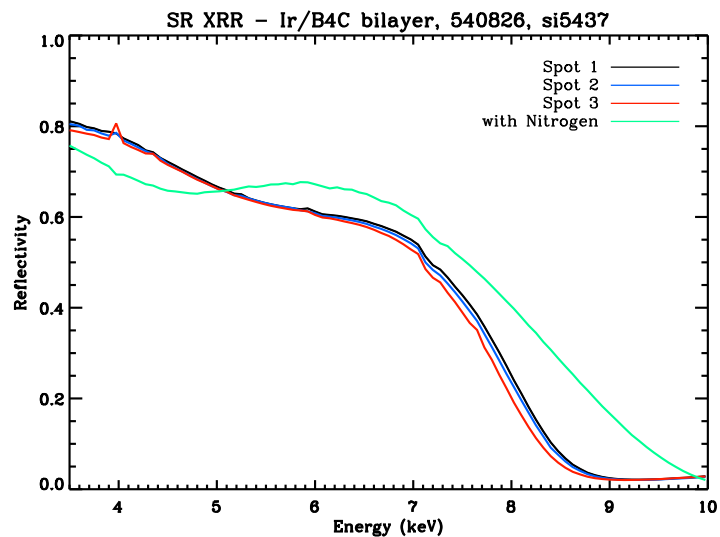
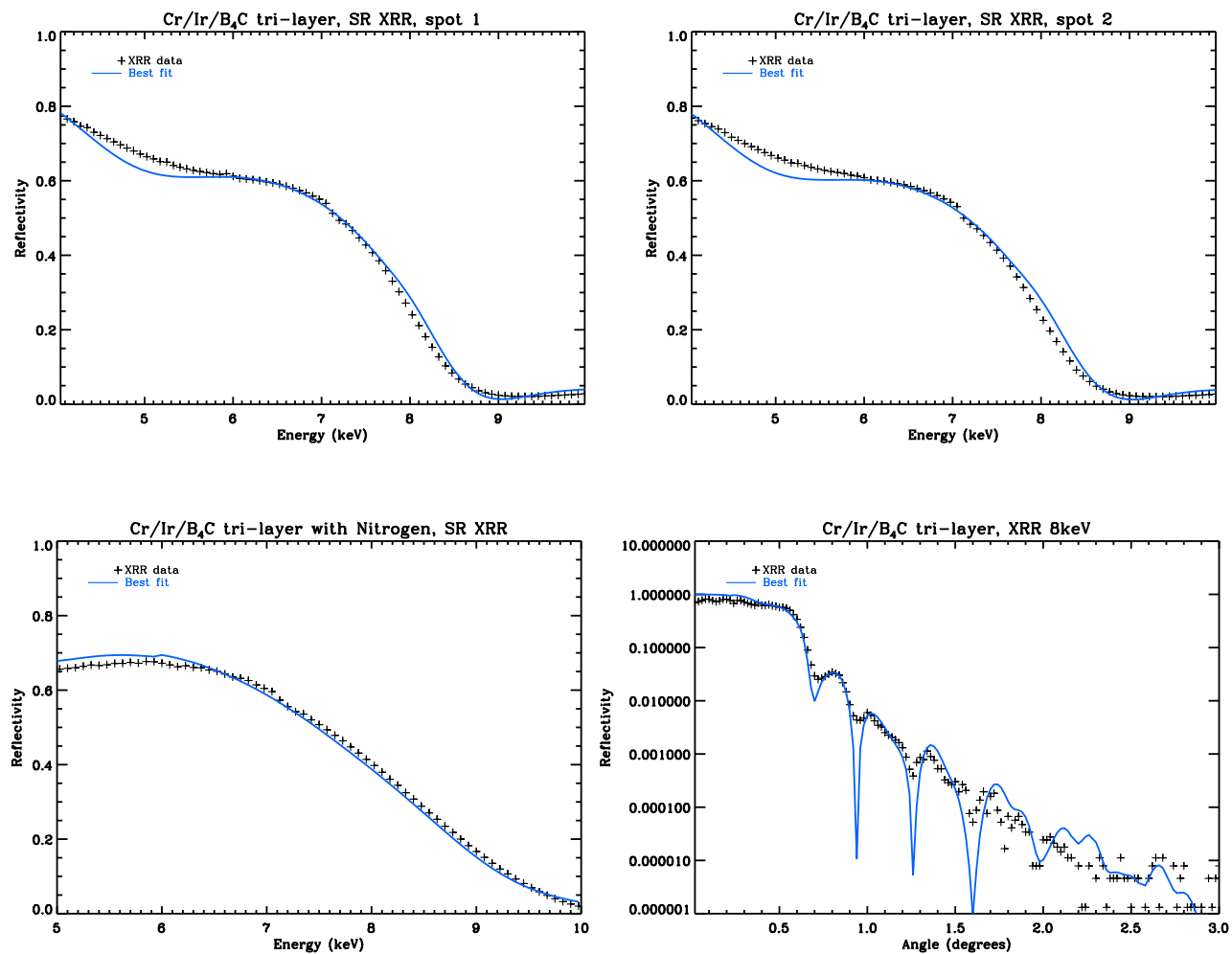Figure 12. Synchrotron Radiation XRR data, tri-layer Cr/Ir/B$_4$C.

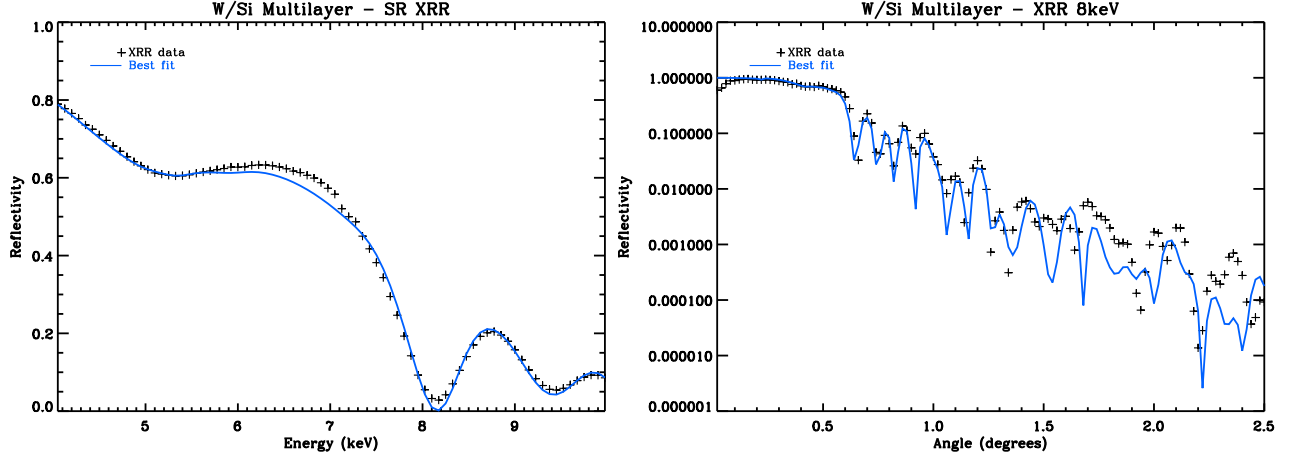

Figure 13. XRR data and best-fit model, tri-layer Cr/Ir/B$_4$C.

Figure 14. XRR data and best-fit model, multilayer W/Si.

	n	Γ	d_{min} (nm)	d_{max} (nm)	d_W (nm)	d_{B_4C} (nm)
Coating recipe[2]	5	0.60	5.0	11.0	11.0	8.0
Best-fit values	5	0.62	4.5	11.2	10.4	10.4
Offset	-	3.23%	10.00%	1.82%	5.40%	30.00%

Table 4. Linear graded W/Si multilayer. Listing model and best-fit values for number of bi-layers (n), thickness ratio between heavy and light material (Γ), minimum bi-layer thickness (d_{min}), maximum bi layer thickness (d_{max}), thickness of the W cap layer (d_W), and thickness of the B_4C overcoat d_{B_4C}

3.5 Multilayer coating development and tests

In addition to the baseline, an multilayer coating of W/Si[2] was also produced and submitted to the coating characterization processes described above. The multilayer coating consists of five W/Si bi-layers with a cap layer of W on top of the bi-layers and a overcoat of B_4C. The W/Si multilayer coating had a successful adhesion test, and presented low stress, $\approx$ -400 MPa.

Coating characterization using XRR was performed on the W/Si multilayer. As described in 3.1, the XRR data collected at the laboratory of PTB at BESSY II and at the 8 keV X-ray facility at DTU Space. The XRR data was fit in order to the optimized coating model using IMD. The model parameters allowed to vary are: layer thickness for each individual layer, thickness ratio between heavy and light material (Γ) and roughness for each layer interface.

The XRR data along with the best fit curves is presented in figure 14. The coating model, best-fit values and the offset between model and best-fit values are listed in table 4. The discrepancies between the coating recipe and best-fit values are due to the calibration procedure. An average roughness of 0.525 nm was obtained by fitting a model to the W/Si XRR data.

To image the layer structure, cross-sectional Transmission Electron Microscopy (TEM) was performed on the coated SPO sample containing the W/Si multilayer. A small section of the coated plate is cleaved and thinned by a focused ion beam milling.[11, 12] The samples must be thin enough in order to be transparent to electrons, the sample thickness for this analysis is less than 100 nm.

The TEM image of the W/Si multilayer coating is shown in figure 15. Further coating characterization includes a complete TEM study where we expect to evaluate the individual coated layers and their interface roughnesses. The TEM study is ongoing and will be reported in the near future.

4. SUMMARY

The performance of the mirror coatings plays a critical role for the ATHENA mission. In this study, we have presented the initial results on the testing for development and characterization of coatings on SPO substrates.
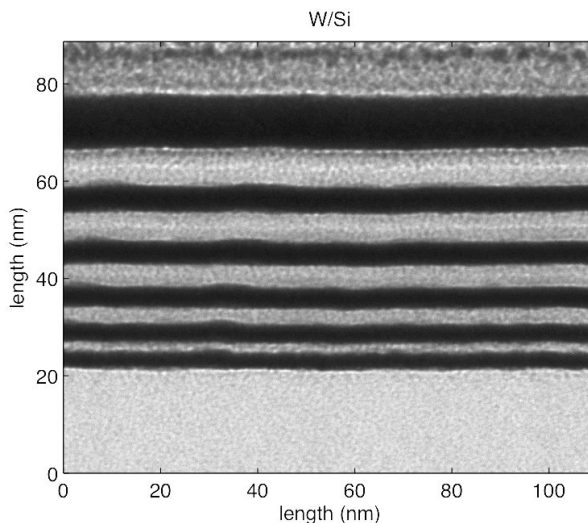
Figure 15. TEM image of the W/Si multilayer coating.

We performed pre-coating characterization on the SPO substrates making use of both AFM and XRR measurements. The AFM measurements of SPO substrates with resist stripes present structures consistent with particulate contamination. A complete AFM study is being performed in order to, among other things, verify this results. XRR measurements indicate that the wedge deposition increases the substrate surface roughness by $\approx 80\%$. The resist stripes further increases the roughness by $\approx 11\%$. Initial scatter measurements indicate little or no scattering on uncoated SPO substrates.

We performed coating characterization on both the baseline Ir/B_4C bi-layer and on a optimized W/Si multilayer coating. We tested the use of Cr as an undercoat to reduce the high stress on the Ir/B_4C bi-layer. We find that introducing a bottom layer of Cr does indeed reduce the coating stress, but increases the surface roughness by 30%, with derived values for the surface roughness of Cr/Ir/B4C tri-layer reaching 0.65 nm.

We investigated the introduction of N_2 gas during sputter deposition to reduce stress and roughness. We observe significant reduction in the Ir/B_4C interface roughness while the coating stress showed no improvement. Further studies are necessary to assess the impact of N_2 gas on the coating performance.

The W/Si multilayer coating tested seems to perform well and shows low stress. The coating is well fit by the optimized IMD model,[2] with average roughness of 0.525 nm.

The development and characterization of coatings on SPO substrates is rapidly progressing and new results on both preliminary characterization and further investigation of other material combinations will be reported in the near future.

REFERENCES

[1] Wallace, K., Bavdaz, M., and Gondoin, P., "Silicon pore optics development," *Proceedings of SPIE* **7437** (2009).

[2] Ferreira, D. D. M., Christensen, F. E., Jakobsen, A. C., Westergaard, N. J. S., and Shortt, B., "ATHENA coating optimization," *Proceedings of SPIE* (2012).

[3] Kofod, N., Garnaes, J., and Joergensen, J. F., "Methods for lateral calibration of Scanning Probe Microscopes based on two dimensional transfer standards in Proceedings of the 4th seminar on Quantitative Microscopy QM 2000 Dimensional measurements in the micro- and nanometre range," *K. Hasche, W. Mirande, G. Wilkening ed. (PTB, Braunschweig, Germany)* , 36–43 (2000).

[4] Windt, D. L., "TOPO - Surface topography analysis, version 2.05," (Sept. 2000).

[5] Krumrey, M. and Ulm, G., "High accuracy detector calibration at the PTB four-crystal monochromator beamline," *Nucl. Instr. and Meth. A* **1175 - 1178**, 467 – 468 (2001).

[6] Yoneda, Y., "Anomalous surface reflection of x-rays," *Physical Review* **131**, 2010 (1963).

[7] Windt, D., "Reduction of stress and roughness by reactive sputtering in W/B4C X-ray multilayer films," *Proceedings of SPIE* **6688** (2007).

[8] Hill, M., Blake, P., Carter, R., Wing-Chan, K., and Deere, K., "International X-Ray Observatory (IXO) Segmented Glass Mirror Technology Development Status And Roadmap," tech. rep. (Sept. 2010).

[9] Jakobsen, A. C., Ferreira, D. D. M., Christensen, F. E., Shortt, B., Collon, M., and Ackermann, M. D., "Preliminary coating design and coating developments for ATHENA," in [*Optics for EUV, X-Ray, and Gamma-Ray Astronomy V*], SPIE (Sept. 2011).

[10] Windt, D. L., "IMD - Software for modeling the optical properties of multilayer films," *Computers in Physics* **12**, 360–370 (Jan. 1998).

[11] Williams, D. B. and Carter C. B., [*Transmission electron microscopy : a textbook for materials science.*], Springer, New York London (2009).

[12] Brejnholt, N. F., [*NuSTAR calibration facility and multilayer reference database*], The Technical University of Denmark (2012). Ph. D. Thesis.